Photochemical & Photobiological Sciences (2022) 21:1159–1173
https://doi.org/10.1007/s43630-022-00197-0

ORIGINAL PAPERS

Comparing deep eutectic solvents and cyclodextrin complexes as curcumin vehicles for blue-light antimicrobial photodynamic therapy approaches

Eduardo Silva[1,2] · Ivo M. Aroso[1,2] · Joana M. Silva[1,2] · Rui L. Reis[1,2]

Received: 1 December 2021 / Accepted: 26 February 2022 / Published online: 2 April 2022

Abstract

Curcumin (Cur), a polyphenolic compound derived from *Curcuma longa* L., has garnered the attention of the scientific community due to its remarkable biological properties such as its potential as a photosensitizing agent for photodynamic therapy (PDT). However, due to its low solubility in aqueous media and instability at physiological and alkaline pH, Cur has struggled to find relevant clinical application. To tackle these shortcomings, two distinct Cur-based formulations based on either complexation with methyl-β-cyclodextrin (MβCD), MβCDC-Cur, or dissolution in a choline chloride (ChCl): glycerol (Gly) deep eutectic solvent (DES), DES-Cur, were produced, physio-chemically characterized and compared regarding their potential as phototherapeutic agents for blue-light antimicrobial photodynamic therapy (aPDT) approaches. Both MβCD-Cur and DES-Cur were able to greatly enhance Cur solubility profile when compared to Cur powder. However, MβCD-Cur appears to hinder some of Cur's basal biological properties and possessed greater basal cytotoxicity towards L929 murine fibroblast cell line. Furthermore, MβCD-Cur was less photo-responsive when exposed to light which may hamper its application in blue-light aPDT approaches. In contrast, DES-Cur showed good biological properties and high photoresponsivity, displaying relevant phototoxicity against bacterial pathogens (≥ 99.9% bacterial reduction) while being better tolerated by L929 murine cells. Overall, this study found DES to be the more effective vehicle for Cur in terms of phototherapeutic potential which will serve as basis to develop novel platforms and approaches for blue-light aPDT targeting localized superficial infections.

Graphical abstract

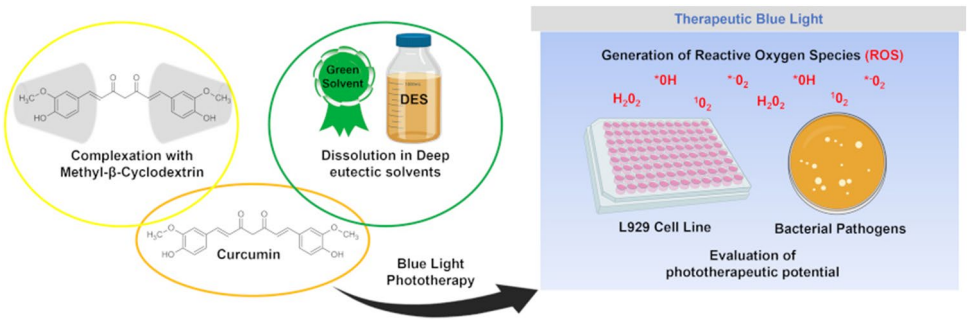

Keywords Curcumin · Photosensitizer · Photodynamic therapy · Deep eutectic solvents · Cyclodextrin · Antimicrobial · Phototoxicity

1 Introduction

Throughout history, natural compounds have been major players in the medical field as both therapeutic agents themselves and/or as source of inspiration for novel synthetic

✉ Joana M. Silva
joana.marques@i3bs.uminho.pt

Extended author information available on the last page of the article

drugs [1, 2]. Among these Curcumin (Cur), a polyphenolic compound derived from the rhizomes of the *Curcuma longa* L., has garnered the attention of the scientific community due to its remarkable biological potential (e.g., anticarcinogenic; antioxidant; antimicrobial; among others) and versatility [3, 4].However, due to its poor water solubility and instability in neutral-alkaline pH, Cur has struggled to find relevant application in modern medicine [5, 6]. Nevertheless, several studies have highlighted Cur's potential as a photosensitizer for photodynamic therapy (PDT) aimed at the treatment of infections, cancer or hyperproliferative skin disorders [7–10].

PDT can be summarized as an oxygen-dependent photochemical reaction that leads to cell death [11]. This process is mediated by the activation of a photosensitizing agent, which upon exposure to light leads to the generation of cytotoxic reactive oxygen species [12]. This technique has shown great promise as an alternative to classic approaches for infection treatment (i.e., antibiotics), in an age where multidrug-resistant pathogens are becoming increasingly common [8, 11, 12]. Nevertheless, it is still plagued by issues regarding its application, such as the lack of selectivity and low water solubility of many potential photosensitizers, as well as safety concerns due to sometimes requiring the application of UV radiation, which is tied to several harmful effects in the human body [11, 13, 14].

In this context, Cur possesses some advantages since it requires blue-light activation, which is inherently more biocompatible than UV radiation, to display its phototherapeutic effects, is easy to handle and cost efficient [7, 8]. Additionally, since blue-light displays low tissue penetration it is well suited for the treatment of localized surface infections as it minimizes photodamage to surrounding tissues. Consequently, improving the solubility and stability of Cur would greatly enhance its effectiveness not only as a photosensitizer but as an overall active pharmaceutical ingredient (API) [5–7]. As such, several attempts were made to improve Cur solubility [6, 15–18].

A particularly successful method was the inclusion of Cur in cyclodextrin (CD) complexes [16, 18]. CDs are a family of cyclic oligosaccharides, normally obtained from starch via enzymatic conversion which can be divided into three main groups namely, α-CD; β-CD and γ-CD [19]. Due to its hydrophobic pocket, CD can form complexes with hydrophobic compounds, such as Cur, greatly enhancing their solubility and overall stability [16, 18]. However, previous studies show that complexation of Cur with β-CDs protects Cur from the effects of light which may hinder a PDT approach [16, 20].

Recently, deep eutectic solvents (DES) have also been studied as a possible alternative for the improvement of Cur's solubility and biological performance [21, 22]. A DES is produced by mixing two or more compounds, that at a certain molar ratio will display an acute decrease of their melting points when compared with the parent compounds [23]. While this phenomenon is majorly attributed to the establishment of hydrogen bonding interactions between the compounds it has been postulated that other forces (i.e., electrostatic interactions; van der Waals forces) may play a role in DES supramolecular arrangement [23, 24]. DES comply with several of the 12 green principles proposed by Paul Anastas and John Warner and have been utilized as an alternative to organic solvents for various purposes, such as carriers for different APIs being designated in this instance as therapeutic deep eutectic solvent (THEDES) [25–30]. Recent studies have highlighted the potential of DES as effective solubilizers of Cur, with choline chloride (ChCl) and glycerol (Gly) DES showcasing great effectiveness [21, 22].

As such, considering the vast potential of these systems for biological applications, this study carried out a comparative performance analysis between methyl-β-cyclodextrin (MβCD)-based, MβCD-Cur, and DES-based, DES-Cur, Cur formulations regarding phototoxicity against pathogenic agents. Ultimately, it is expected that complexation with MβCD and dissolution in DES leads to greater solubilization of Cur while also facilitating its diffusion through biological membranes culminating in the conception of organic solvent-free Cur-based formulation with phototherapeutic potential for novel PDT approaches.

2 Materials and methods

2.1 Production of DES-Cur and MβCD-Cur formulations

To produce DES-Cur, firstly ChCl (ref. C1879, Sigma-Aldrich) was mixed with Gly (99% puriss, ref. 15,523, Sigma-Aldrich) at a 1:1.5 molar ratio. The mixture was stirred (80 RPM) under heating at 80 °C until a clear solution was formed. Posteriorly, an excess of commercial Cur (200 mg) (95% ≥ Total Curcuminoids, 94% Cur, 3% demethoxycurcumin, 3% bisdemethoxycurcumin, ref. B21573, Alfa Aesar) was added to 25 mL of ChCl:Gly DES and left dissolving at 37ºC 180 RPM for 72 h. Finally, the mixture was centrifuged at 16,639×*g* using an Eppendorf 5810R (Eppendorf, Germany) for 1 h and supernatant collected and stored at room temperature (RT) (25 °C) protected from light.

MβCD-Cur was prepared as elsewhere reported [31]. Briefly, MβCD (1.7 molar substitution, ref. 779,776, Sigma-Aldrich) was mixed with Cur at a 2:1 molar ratio and macerated for 15 min. Posteriorly, small volumes of ethanol (EtOH) 50% (v/v) were added and mixed until a thick homogeneous paste was formed, followed by an additional hour of maceration. Finally, the obtained paste was dried at

45 °C in a Vacuum oven (VD23, Binder) and ground into a fine powder. The obtained complex was then stored at RT and protected from light.

2.2 Differential scanning calorimetry (DSC)

Experiments were performed using the DSC Q100 Thermo analyzer (TA instruments, USA), in an aluminum pan. Approximately, 5 mg of either MβCD-Cur (powder) or DES-Cur (liquid) were weighed into the pan to conduct the experiment. The program applied consisted of an initial heating step from − 20 to 200 °C (heating rate 10 °C min^{-1}), followed by an isothermal step of 2 min, and a final cooling step to − 20 °C (cooling rate 10 °C min^{-1}). Experiments were performed under a nitrogen atmosphere (purge gas flux of 50 mL min^{-1}) in triplicate.

2.3 Viscosity measurements

The viscosity measurements were performed using a Kinexus Prot Rheometer (Kinexus Prot, MaL 1,097,376, Malvern Instruments, USA) fitted with a parallel plate geometry (PU20 SR1740 SS) with a 1 mm gap. Measurements were performed under controlled stress conditions with a shear rate of 10 s^{-1}. Shear viscosity was determined over a temperature range of 20°–50 °C with a ramp of 2 °C/min.

2.4 Attenuated total reflection Fourier Transformed Infrared (ATR-FTIR) spectroscopy

FTIR measurements were recorded using a IRPrestige-21 spectrophotometer (Shimadzu, Japan), by averaging 32 independent scans, in a wavenumber range of 600–4500 cm^{-1} and a resolution of 2 cm^{-1}. Spectra processing was carried out using IRsolution© 1.20 software (Shimadzu, Japan) and Origin® 2018 (OriginLab, USA).

2.5 Powder X-ray diffraction (XRD)

MβCD-Cur was analyzed by XRD using a Bragg–Brentano diffractometer (Bruker D8 Advance DaVinci, Germany) equipped with CuKα radiation. Data sets were collected scanning between 5° and 35° 2θ at 8°/min with a 0.04° step size.

2.6 Cur solubility measurements

The amount of Cur present in both formulations was evaluated by UV–visible spectroscopy using a SYNERGY HT microplate reader (BioTek Instruments, USA). For MβCD-Cur, firstly saturated solutions were prepared in two different buffers namely, PBS 7.4 pH (ref. P4417, Sigma-Aldrich) and MES 0.5 M pH 6.0 (ref. M8250, Sigma-Aldrich), by adding an excess of conjugate (500 mg) to 20 mL of buffer, followed by stirring (80 RPM) at RT overnight. Prior to quantification, the saturated solutions of MβCD-Cur were filtered using 0.22 µm PES syringe filters to remove undissolved complex and pH values registered. For absorbance measurement at 425 nm, serial dilutions of MβCD-Cur saturated solutions and DES-Cur formulation were prepared using EtOH. Cur concentration was obtained by extrapolation using a linear regression built with Cur standards at a concentration range of 100–1.563 µg/mL considering the dilution factor. The amount of Cur on saturated solutions of PBS pH 7.4; MES 0.5 M pH 6.0; deionized water; pure Gly and aqueous solutions of the individual DES components were also determined to evaluate Cur solubility enhancement. Finally, Cur solubility in aqueous solution of DES-Cur was also assessed. Briefly, aqueous solution of DES-Cur was prepared in MES 0.5 M pH 6.0 buffer with dilution factors (DF) ranging from 2 to 100, followed by incubation under stirring (80 RPM) at 37 ºC for 3 h. After incubation, samples were centrifuged at 16,639×*g* for 60 min to remove any resulting precipitates, pH values were then measured and finally Cur content quantified as described above. Posteriorly, the UV–visible quantification values were confirmed by HPLC–MS adapting a previously reported method [32]. Further information regarding HPLC–MS quantification can be found in the supporting information. All measurements were done in triplicate and three independent quantifications were performed for each sample.

2.7 Determination of antioxidant potential

The ability of the formulations to preserve Cur antioxidant capacity (i.e., DES-Cur; MβCD-Cur- in PBS and MβCD-Cur in MES) were evaluated over a period of 14 days, when stored at RT and protected from light. The assay was performed using 2,2-diphenyl-1-picrylhydrazyl (DPPH, ref D9132, Sigma-Aldrich), as elsewhere reported [33]. Briefly, at predetermined timepoints (1, 3, 7 and 14 days) the formulations were serially diluted using EtOH to equivalent Cur concentrations of 50, 25, 12.5, 6,25 and 3.125 µg/mL. The prepared dilutions were then added to a DPPH stock solution prepared in EtOH at a 7:3 volume ratio. After 30 min of incubation (RT, 80 RPM), absorbance was read at 517 nm using a SYNERGY HT microplate reader (BioTek Instruments, USA). The half maximum effective concentration (EC_{50}) was determined by plotting scavenging activity against the Cur concentration.

2.8 Determination of Cur-based formulations photo-responsiveness

The photo-responsiveness of an aqueous solution of DES-Cur and MβCD-Cur was evaluated using a home-made

illumination device equipped with an OSRAM Dulux S Blue 9 W/71 Lamp (OSRAM GmbH, Germany) with an estimated radiated power of 2.3 W at a spectral range of 400–550 nm. Power density at sample location was measured and found to be 5.12 mW/cm^2 using a NIST-calibrated light radiometer. The spectral distribution of the used lamp (Fig. S1) as well as a schematic representation of the device is included in the supplementary information (Fig. S2). Prior to irradiation the absorbance spectra, between 380 and 600 nm, of ChCl:Gly DES, MβCD (5 mg/ml in ddH_2O), Cur in EtOH (25 µg/ml), as well as dilutions of DES-Cur and MβCD-Cur in MES 0.5 M pH 6.0 buffer with an equivalent Cur concentration (25 µg/ml) were obtained using a SYNERGY HT microplate reader (BioTek Instruments, USA). Posteriorly, the aqueous solutions of the formulations and Cur in EtOH were irradiated with varying energy densities (1.54, 6.15, 12.30, 18.43 and 23.04 J/cm^2) using the above-described apparatus. Photo-responsiveness was inferred via monitorization of Cur consumption by absorbance measurement at 425 nm using a SYNERGY HT microplate reader (BioTek Instruments, USA). Effective Energy Density (EED50), defined has the required energy density to consume 50% of Cur in solution, was obtained by plotting the percentage of Cur consumed against applied energy density.

2.9 Antibacterial activity and phototoxicity against bacterial pathogens

Antibacterial and phototoxicity of the formulations were evaluated against clinically relevant pathogens, namely *Escherichia coli* ATCC 25,922 and *Staphylococcus aureus* ATCC 25,923. Firstly, an initial screening was performed via Disk Diffusion Assay (DDA) as reported elsewhere [27]. Briefly, DES-Cur, MβCD-Cur formulations and raw components (approximately 25 mg) were loaded into a paper disk and placed onto Mueller–Hinton Agar (ref. X926, Carl Roth), previously streak inoculated using a bacterial suspension with approximately $0.5–1.5\times10^8$ CFU/mL. Plates were then incubated for 24 h at 37 ºC, followed by measurement of the inhibition halo. Posteriorly, Minimum inhibitory concentration (MIC) and Minimum bactericidal concentration (MBC) were determined for planktonic cultures of these pathogens, using previously reported methods [27]. Briefly, serial dilutions (500–1.25 mg/ml) of the formulations were prepared in Mueller–Hinton broth (ref. 70,192, Millipore) and incubated for 24 h (37ºC 180RPM) with a bacterial suspension of approximately $0.5–1.5\times10^6$ CFU/mL. After incubation, the suspension was replated into tryptic soy agar (TSA) (ref. 610,053, Liofilchem) and incubated for 24 h at 37ºC.

To assess phototoxicity, sub-MIC concentrations of DES-Cur (100 µL were mixed with an equal volume of bacterial suspension ($0.5–1.5\times10^6$ CFU/mL) in a 96-well plate (Corning, Ref. 353,072). Posteriorly, the suspensions were irradiated (9.22 J/cm^2) using the previously described homemade illumination device. After irradiation, 10 µL drops are placed onto TSA plates and incubated for 24 h. The concentration where no bacterial growth was observed was considered the minimum phototoxic concentration (MPC). Additionally, kinetic studies centered around the determined MPC were also performed by varying energy densities (1.54, 3.07, 4.61, 9.22 and 13.82 J/cm^2). Following light irradiation, samples were serially diluted ($10^0–10^{-6}$), 100 µL spread onto TSA plates and incubated at 37 °C for 24 h. Finally, bacteria colonies were counted and Log_{10} reduction calculated. All procedures were carried out using three independent bacterial inoculations to account for biological variance.

2.10 Determination of Cytotoxic and phototoxic effect against L929 Cell line

The cytotoxicity of all the formulations against animal cells was evaluated using L929 murine fibroblast cell line according to ISO/EN 10,993 guidelines. Briefly, dilutions of DES-Cur, MβCD-Cur and raw materials were prepared using Dulbecco's Modified Eagle Medium (DMEM, ref. D5523, Sigma-Aldrich) (126–0.001 mg/mL) and 200 µL added to previously established cell monolayers (10 000 cells/well) in a 96-well tissue culture plate followed by incubation for 24 h. Possible morphology changes were observed by optic microscopy (AxiovertA1, Zeiss). Posteriorly, cell viability was assessed by MTS (ref. G3581, Promega) colorimetric assay at a wavelength of 490 nm. EC_{50} was calculated by plotting formulation/compound concentration against cell viability. To evaluate the phototoxic effect, cells were exposed to the MPC values, followed by light exposure at varying energy densities (1.54, 3.07, 4.61, 9.22 and 13.82 J/cm^2). Cells were then observed using an inverted microscope (CKX53, Olympus). Prior to being subjected to a live/dead assay cells were washed twice with PBS to remove any vestigial Cur that may interfere with fluorescence image acquisition. Cells were then stained with 2 µL of Calcein AM (Ex_λ/Em_λ 494/517 nm) and 1 µL of Propidium iodide (Ex_λ/Em_λ 536/617 nm) for 20 min. Cells were then visualized using an inverted fluorescence microscope (Axio observer, Zeiss).

3 Results and discussion

3.1 Preparation and characterization of Cur-based formulations

In this work, formulations of Cur using two different vehicles were produced and evaluated regarding their potential

as phototherapeutic agents. The visual aspect of the formulations at RT is presented in the supplementary information (Fig. S3). To characterize the produced formulations firstly. a DSC analysis was carried out to evaluate thermal events and infer upon established interactions between the individual counterparts (Fig. 1).

Observing the obtained thermograms one can verify endothermic events in the raw materials Cur and ChCl at temperatures 177.74 °C and 75.01 °C, respectively. These endothermic peaks are characteristic of these compounds being in accordance with previous reports in the literature [31, 34]. Looking at the thermogram of DES, a suppression of the endothermic event of ChCl was observed. This can be attributed to intermolecular interactions established with the other DES component, Gly, suggesting a supramolecular rearrangement which results in a loss of lattice arrangement while the compounds are in eutectic form [35, 36]. Looking at the thermogram of DES-Cur, one can verify the suppression of Cur endothermic peak suggesting its integration in the DES supramolecular structure, a phenomenon which has been previously reported [34, 36, 37]. When analyzing MβCD-Cur's thermogram, a suppression of Cur's endothermic peak is also observed indicating the formation of a MβCD-Cur complex, at a 2:1 molar ratio, with Cur becoming entrapped in MβCD hydrophobic cavity [31].

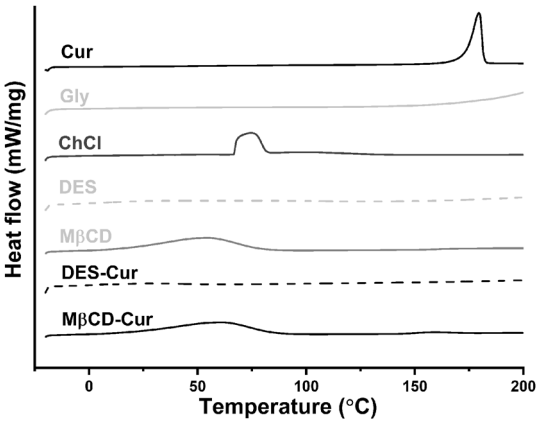

Fig. 1 DSC Thermograms of DES-Cur, MβCD-Cur and raw materials. Peaks above baseline correspond to endothermic events

Posteriorly, ATR-FTIR analysis was carried out to gain further insights into the molecular interactions' resultant from dissolution or complexation of Cur in/with DES and MβCD, respectively (Fig. 2).

Firstly, when comparing the spectra of the DES raw components (i.e., Gly and ChCl) with DES itself (Fig. 2A), it is possible to observe an upshift of peaks from 2932 and 2874 cm^{-1}, belonging to Gly, ascribed to C-H stretching, to 2975 and 2900 cm^{-1}, which confirms changes in molecular environment resultant, most likely, from eutectic interactions [38, 39]. Furthermore, an upshift of two peaks belonging to ChCl can also be observed. The peak centered at 1325 cm^{-1},ascribed to CH_2 twist, N–C asymmetric stretching suffers an upshift to 1402 cm^{-1}, while the peak centered

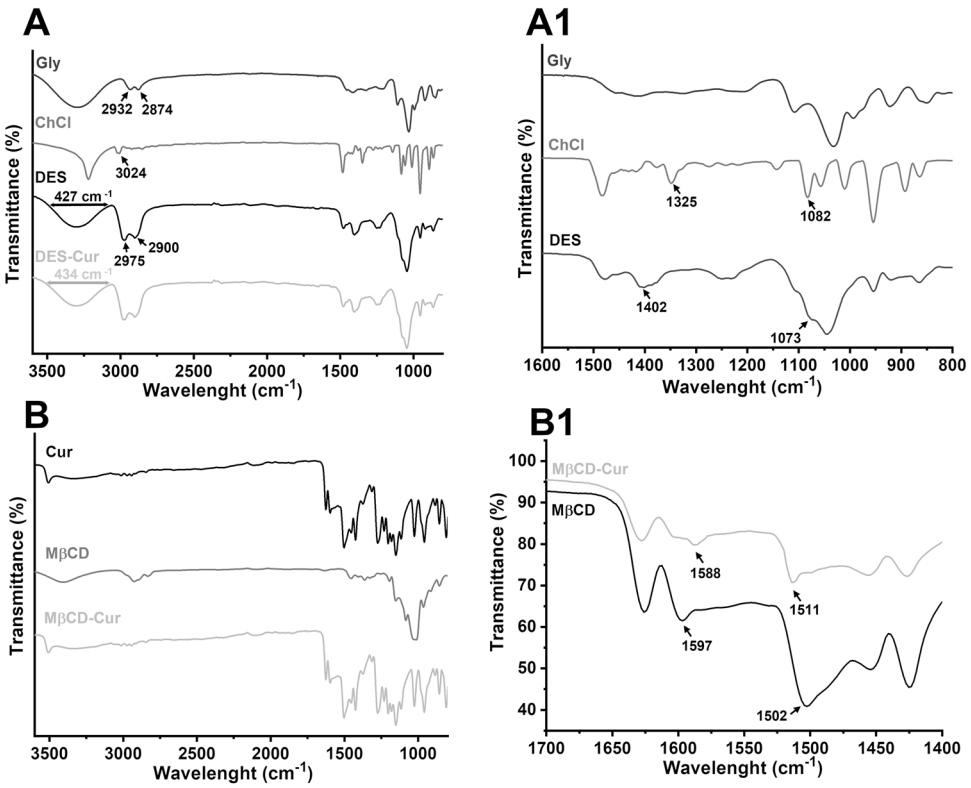

Fig. 2 **A** ATR-FTIR spectra of Gly, ChCl, DES and DES-Cur. **A1** Zoom of 800–1600 cm^{-1} region of Gly, ChCl and DES. **B** ATR-FTIR spectra of MβCD, MβCD-Cur and Cur. **B1** Zoom of 1400–1700 cm^{-1} region of MβCD-Cur and Cur

at 1082 cm^{-1}, ascribed to CH_2–CH_2−O stretch vibration, suffers a downshift to 1073 cm^{-1}(Fig. 2A1) further suggesting the establishment of H-bonds between ChCl and Gly [40, 41]. Additionally, the peak belonging to ChCl at 3024 cm^{-1}, ascribed to N–H stretching, is not visible in the DES spectra (Fig. 2A) which has been previously reported for several ChCl-based DES [42]. When comparing the spectra of DES-Cur with DES, it becomes evident that they almost fully overlap with no immediate clear differences. The characteristic peaks of Cur cannot be detected due to a masking effect caused by the strong peak intensity of the DES components and establishment of intermolecular interactions. Similar behavior has been previously observed for DES containing β-carotene [43]. Nevertheless, slight differences can be observed between the two spectra (Fig. 2A). In the peak centered around 3302 cm^{-1} associated with O−H stretching, a broadening of approximately 7 cm^{-1} in the spectra of DES-Cur is seen when compared with that of DES. This evidence suggests an alteration of DES network, possibly due to the introduction of Cur and its interaction with the DES supramolecular structure [38, 41, 44]. When comparing the spectra of MβCD and MβCD-Cur (Fig. 2B) it is possible to verify that the spectrum of MβCD-Cur displays prominent peaks from both individual components, although it is overall alike the spectrum of MβCD. In the 1400–1700 cm^{-1} region, a shift in two peaks belonging to Cur can be observed (Fig. 2B1). These shifts, previously reported by *Mangolin* et al., occur at 1502 cm^{-1} corresponding to C=O and C=C vibrations, which undergoes an upshift to 1511 cm^{-1} and at 1597 cm^{-1} corresponding to the stretching vibrations of the benzene ring, suffering a downshift to 1588 cm^{-1}. These occurrences most likely result of Cur's interactions with MβCD hydrophobic pocket and provide additional evidence of complexation [16, 45].

The shear viscosity of the DES, DES-Cur and aqueous solution of MβCD-Cur were assessed by rheology (Fig. S4) as this parameter should be considered when conceptualizing specific applications (i.e., topical application, inclusion in a solid support) to guarantee a satisfactory dosage/release of bioactive molecules into the site of interest. As expected, the aqueous solution of MβCD-Cur shows negligible shear viscosity with no apparent variation with increasing temperature. Regarding the eutectic formulations, DES-Cur shows a slightly higher viscosity than the DES with both systems suffering a significant decrease of viscosity increasing temperature [46] which is in accordance with the principles postulated by the Arrhenius equation. The slightly higher viscosity of DES-Cur is likely a consequence of the added presence of Cur since the viscosity will depend on the constituents of the system. Several other studies have described similar behavior for eutectic formulations where viscosity was tailored by several factors such as water content and chemical composition [47, 48]. Additionally, XRD spectroscopy was also carried for MβCD-Cur, Cur and MβCD in solid state (Fig. S5). Cur displays characteristic peaks that point to the crystalline nature of the compound. However, these peaks are not present in the MβCD-Cur spectrum, suggesting both the formation of an inclusion complex between MβCD and Cur with the adoption of an amorphous state [31].

Finally, the solubility of Cur in each formulation, typical polar solvents, individual DES components and aqueous solutions of DES were determined (Table 1).

Observing the values reported in Table 1 it becomes evident that the amount of Cur present in both DES-Cur and MβCD-Cur formulations is drastically superior to those obtained by simply dissolving Cur in aqueous solvents. Solutions of MβCD-Cur in MES and PBS show a high Cur content proving to be effective solubilizers, enhancing Cur aqueous solubility by over 2000x. The pH values of saturated solutions of MβCD-Cur (MES) and MβCD-Cur (PBS) were 6.09 and 7.36, respectively. Curiously, the amount of Cur in the two buffers used to prepare conjugate solutions is not significantly different. Previous accounts in the literature report that Cur is more soluble, although also more prone to degradation, in higher (alkaline) pH levels. Likewise, it is also reported that Cur is less soluble at lower (acidic) pH levels although it is much more stable [5, 49]. Consequently, the similarity of Cur amount in both PBS and

Table 1 Cur solubility in the developed formulations, polar solvents, individual DES components and aqueous solutions of DES-Cur

Formulations	[Cur] (mg/mL)
MβCD-Cur (MES)	3.23 ± 0.46
MβCD-Cur (PBS)	3.35 ± 0.35
DES-Cur	7.21 ± 0.20
Solvents	
Water	0.0011 ± 0.0001
MES	0.0012 ± 0.0001
PBS	0.0011 ± 0.0003
Individual DES components	
Gly (pure)	0.80 ± 0.04
Gly aqueous[α]	0.06 ± 0.04
ChCl aqueous[α]	0.16 ± 0.06
Aqueous solution of DES-Cur	
DF 2	0.67 ± 0.04
DF 4	0.078 ± 0.002
DF 10	0.019 ± 0.00025
DF 20	0.012 ± 0.00021
DF 40	0.011 ± 0.00025
DF 100	0.0101 ± 0.00103

DF dilution factor

[α]Composition of these aqueous solutions were based on the molar ratios of the counterparts, substituting the mass of one component with water

MES solutions of MβCD-Cur becomes another evidence of complexation, as the inclusion of Cur into MβCD hydrophobic pocket partially protects Cur from the effects of the surrounding environment's pH [16]. The eutectic formulation, DES-Cur shows the greatest amount of solubilized Cur, which is in accordance with previously reports in the literature [21, 31, 50]. Furthermore, the obtained values for the individual components of DES show that the solubilizing capabilities are consequence of the eutectic interactions established between the two components, rather than the result of one individual compound, as previously reported [35]. Finally, the stability of DES-Cur in aqueous media was tested by dilution in MES 0.5 M pH 6.0, resulting in aqueous solution of DES-Cur with pH values between 6.12 and 6.02. As expected, Cur in DES form was much more soluble in aqueous media displaying a solubility enchantment of 558x (DF = 2). In addition, while this effect lessens as the DF rises, it should be noted that even with a DF of 100 an enhancement of 8.43 × in Cur aqueous solubility is observed. This strong solubilization effect may be the result of a phenomenon called hydrotropy [51]. An hydrotrope can be succinctly described as a compound with the ability to increase the solubility of a hydrophobic solute. Even though the exact mechanisms behind hydrotropy are not yet understood, several previous accounts in the literature have ascribed hydrotropic properties to both DES and ionic liquids. It is believed that this phenomenon involves complexation between the solute and hydrotrope, changes in solvent structure or the coaggregation of the solutes with the hydrotrope [52–54].

3.2 Antioxidant capabilities and photo-responsiveness of Cur-based formulations

Beyond solubilizing capabilities, it is also important that the herein developed formulations allow Cur to retain, over storage time, its biological properties. As such, antioxidant potential was measured at specific time points and compared with Cur standards prepared in EtOH, since Cur presents high stability in this solvent [55] (Table 2).Furthermore, studies using blank DES and a MβCD aqueous solution were also conducted, but no relevant antioxidant capability was found at the tested concentration range.

The results obtain show that throughout the 14-day period, Cur contained in DES-Cur shows the most similar antioxidant activity to the standards, followed by MβCD-Cur (MES) and lastly MβCD-Cur (PBS). This is within expectation since complexation with MβCD may hinder the reactivity of Cur as it is partly protected from interaction with the surrounding environment. Nevertheless, it is expected that the partial dissociation of MβCD-Cur conjugate occurs which may justify the decrease on the antioxidant potential of MβCD-Cur (PBS) when compared with MβCD-Cur (MES), since Cur will suffer greater degradation in alkaline pH [5, 49, 55]. In contrast, MβCD-Cur (MES), although possessing a lower antioxidant potential than DES-Cur, is the formulation most adept at conserving antioxidant potential over time due to the protective effects of complexation with MβCD and the greater stability of Cur at acidic pH. Lastly, the slight decay of antioxidant activity over time in DES-Cur may, partially, be a consequence of the hygroscopic nature of ChCl, resulting in a gradual increase of DES water content possibly leading to Cur degradation [49, 56].

Another key-parameter to evaluate is the photo-response of the formulations since the Cur's efficacy as a photosensitizer depends on its ability to carry out several photochemical processes to induce phototoxicity. Firstly, the absorbance spectra (380–600 nm) of the raw materials, as well as aqueous solutions of the formulations with an equivalent Cur concentration of 25 µg/mL were obtained and compared with an EtOH Cur solution at the same concentration to better understand the photo-response considering the used light source spectral range (400–550 nm) (Fig. 3).

The absorption spectra of Cur shows a broadband maximum absorption peak at ≈ 425 nm wavelength, which can be assigned to low energy π–π^* excitation of Cur and has been previously reported in several studies [57, 58] MβCD-Cur (PBS) displayed the same broadband maximum absorption peak as Cur, while both MβCD-Cur (MES) and DES-Cur showed a very small red-shift of the maximum absorption

Table 2 DPPH free radical scavenging activity of Cur in EtOH and Cur in the various formulations expressed as EC50 values

Formulations	Day 1	Day 3	Day 7	Day 14
DES-Cur	$12.38 \pm 1.02^{\$,\&}$	$12.33 \pm 1.07^{\$,\&}$	$14.30 \pm 1.07^{\$,\&}$	$16.30 \pm 1.18^{*,\&}$
MβCD-Cur (MES)	$16.86 \pm 1.07^{\#,*,\&}$	$17.51 \pm 1.06^{\#,*,\&}$	$17.55 \pm 1.05^{\#,*,\&}$	$17.85 \pm 1.05^{*,\&}$
MβCD-Cur (PBS)	$19.58 \pm 1.05^{\#,*,\$}$	$20.19 \pm 1.06^{\#,*,\$}$	$20.56 \pm 1.07^{\#,*,\$}$	$23.44 \pm 1.11^{\#,*,\$}$
Cur in EtOH	$12.56 \pm 1.08^{\$,\&}$	$13.27 \pm 1.18^{\$,\&}$	$13.15 \pm 1.18^{\$,\&}$	$12.99 \pm 1.12^{\#,\$,\&}$

Statistical analysis (one-way ANOVA) was performed, and differences considered significant for p values < 0.05

#Denotes statistically significant difference when compared with DES-Cur; ($) denotes statistically significant difference when compared with MβCD-Cur (MES); (&) denotes statistically significant difference when compared with MβCD-Cur (PBS);(*) denotes statistically significant difference when compared with Cur

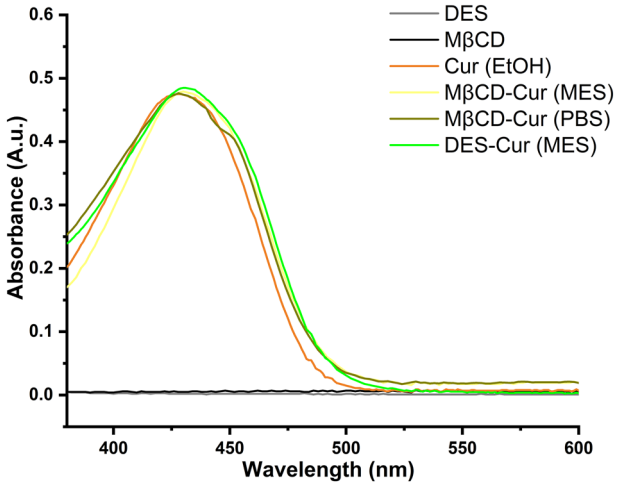

Fig. 3 Absorbance spectra (380–600 nm) of raw materials and aqueous solutions of the formulations

peak to ≈ 428 nm and ≈ 431 nm, respectively which have been previously reported for Cur-based formulations [59, 60]. Regarding DES and MβCD, as expected they displayed no signal response in the spectral range selected. Considering the obtained spectra, it is possible to conclude that the selected light is adequate and that the formulations will be responsive to irradiation with home-made apparatus.

Posteriorly, irradiation at varying energy densities of the formulations was carried out (Fig. 4).

The results obtained show that Cur in EtOH and an aqueous solution of DES-Cur show an equal behavior when exposed to blue-light irradiation, indicating that in a diluted form DES does not appear to affect Cur photo-responsiveness (Fig. 4A). In contrast, MβCD-Cur is heavily resistant to the effects of blue light showing no significant variation in Cur content until up to an energy density of 18.43 which is consistent with previous reports in the literature [61, 62]. The calculated EED_{50} were 11.77 ± 0.31; 23.04 ± 0.32 and 12.57 ± 0.32 J/cm^2 for DES-Cur; MβCD-Cur and Cur, respectively (Fig. 4B). Herein, due to its lower photo-responsiveness MβCD-Cur may not be suitable for blue-light PDT approaches as it will require greater irradiation to trigger its phototherapeutic effect. Nevertheless, to better gauge the potential of the formulations, a robust in vitro assessment of their basal toxicity and phototoxic activity against both relevant bacterial pathogens and a fibroblast cell line was carried out.

3.3 Assessment of the basal cytotoxicity and phototoxic potential of Cur-based formulations against bacterial pathogens and L929 fibroblasts

The basal toxicity of MβCD-Cur in PBS and MES, and DES-Cur (i.e., without blue-light exposure) was assessed against known bacterial pathogens namely *S. aureus* (Gram-positive) and *E. coli* (Gram-negative). Initially, a DDA diffusion assay was carried out (Table S1). After the preliminary DDA assay, MIC/MBC determination was carried out (Table 3).

As can be seen, MβCD-Cur (PBS) shows no antibacterial activity in the concentrations tested and MβCD-Cur (MES) displays very little effect. Overall, complexation with MβCD appears to hinder Cur antibacterial effect. Several reports in the literature point out that Cur's antibacterial properties result of, among other mechanisms, interaction with the bacterial cell envelope [63, 64]. As such, it stands to reason that complexation with MβCD may hinder the antibacterial effect of Cur as it limits its ability to interact with the surrounding environment. Furthermore, the bacterial cell envelope, especially those of Gram-negative bacteria which is comprised of a double-membrane separated by a cell wall, is extremely selective possessing several mechanisms to keep out harmful agents [65, 66]. A Gram-negative bacteria's outer membrane, such as *E. coli*, can possess lipopolysaccharides (LPS), that act as an additional permeability barrier possibly explaining why no antibacterial activity was

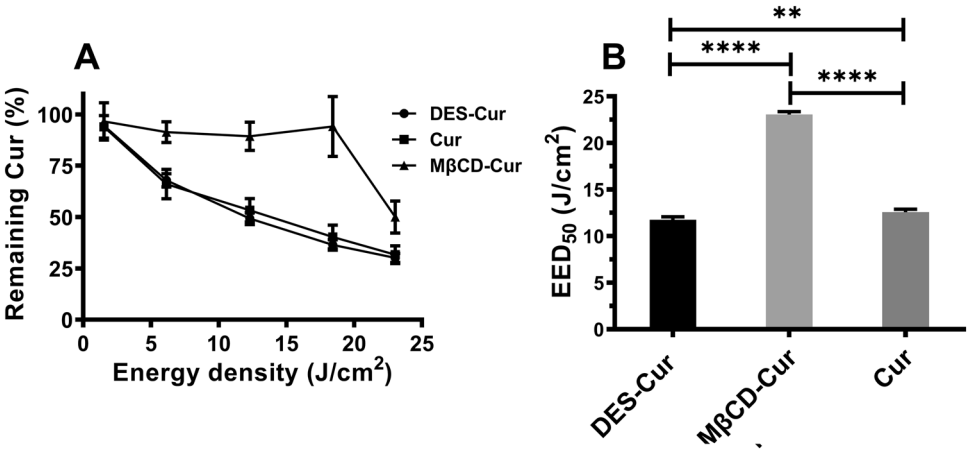

Fig. 4 **A** Photo-responsiveness of DES-Cur, MβC-Cur and Cur at different blue-light energy densities. **B** EED_{50} for Cur-based formulations and Cur. Statistical analysis (one-way ANOVA with tukey post-hoc) was performed: $p < 0.01$(**), $p < 0.0001$ (****)

Table 3 MIC/MBC values of Cur-based formulations and raw materials against *S. aureus* and *E. coli*

Formulations	*S. aureus*				*E. coli*			
	MIC (mg/mL)	[Cur]* (μg/mL)	MBC (mg/mL)	[Cur]* (μg/mL)	MIC (mg/mL)	[Cur]* (μg/mL)	MBC (mg/mL)	[Cur]* (μg/mL)
DES-Cur	5	35.88	10	71.76	5	35.88	10	71.76
MβCD-Cur (MES)	250	837.30	500	1674.60	> 500	> 1674.60	> 500	> 1674.60
MβCD-Cur (PBS)	> 500	> 1562.66	> 500	> 1562.66	> 500	> 1562.66	> 500	> 1562.66
DES	> 50	–	> 50	–	> 50	–	> 50	–
MβCD	> 1000	–	> 1000	–	> 1000	–	> 1000	–
Cur in EtOH[#]	80		≥ 80		> 150		> 150	

*[Cur] present in the amount of formulation employed

[#]Final concentration of EtOH was 5% (V/V%)

verified for *E. coli,* while a minor effect could be seen for *S. aureus* [66–68]. The reason why MβCD-Cur (PBS) displayed no visible antibacterial activity is most likely related to Cur instability at higher pH values which may lead to a poor biological performance due to degradation. Upon measuring the resultant pH of the dilutions of MβCD-Cur (MES) and MβCD-Cur (PBS) in MHB, pH values ranging 6.08–6.17 were obtained for MβCD-Cur (MES) dilutions while for MβCD-Cur (PBS) pH values between 7.36 and 7.42 were registered. As such, a possible cause of MβCD-Cur (MES) antibacterial effect lies in the acidic-shift of pH which does not occur for MβCD-Cur (PBS).

In contrast, an aqueous solution of DES-Cur potentiated Cur's antibacterial activity by more than 2.2-fold, most likely due to an improved bioavailability of Cur when in DES form, as elsewhere reported for other DES systems [34, 60, 65]. This translates in a greater permeation/interaction of Cur with the bacterial cell envelope while included in the DES supramolecular structure, which is consistent with previous reports in the literature where ChCl-based DES increased the permeability of cell membranes and intercellular lipid bilayers [69, 70]. Overall, the results point to DES-Cur as the formulation with the greatest basal antibacterial activity.

The in vitro toxicity of DES-Cur, MβCD-Cur and raw components against L929 murine cell line was also evaluated to infer upon the safety and biocompatibility of the developed formulations (Fig. 5A–C).

Under these conditions the cellular viability showed a dose-dependent response with increasing compound concentration leading to greater loss of cell viability. Using the obtained dose–response curves, the EC_{50} were then calculated (Table 4).

The EC_{50} value of DES-Cur for L929 fibroblasts was shown to be higher than that of MβCD-Cur. This is most likely due to DES, by itself, being less cytotoxic (EC_{50} of 22.59 ± 0.71 mg/mL) than MβCD (EC_{50} of 4.49 ± 0.18 mg/mL), fact which is supported by previous studies [71–74]. Additionally, the results illustrate that the cytotoxic of ChCl:Gly DES differs from the cytotoxicity of its components Gly (EC_{50} of 65.94 ± 2.82 mg/mL) and ChCl (EC_{50} of 10.86 ± 0.60 mg/mL). This suggests that after synthesis the DES display its own characteristic cytotoxicity which is accordance with previous reports [75, 76]. The higher cytotoxicity of MβCD and MβCD-Cur, even though they displayed little to no antibacterial effect, can be easily explained by the difference in membrane structure between bacteria and animal cells. Since animal cells lack the complex cell envelope structure of bacteria, MβCD and MβCD-Cur can more readily interact with the cell membrane resulting in a more pronounced cytotoxic effect. Several accounts in the literature postulate that CDs can extract cholesterol, phospholipids and proteins from cell membranes affecting their structure integrity and permeability [66, 77, 78]. As expected, in concentrations exceeding the EC_{50} a round-like morphology and poor adhesion to well surface was generally observed. In concentrations below the EC_{50}, cells were better distributed upon the well surface displaying a more stretched morphology (Fig. 5D).

Considering the data obtained, DES-Cur showed greater promise as a formulation for blue-light aPDT. Hence, it was selected to carry out the remaining assays focused on the phototoxic potential. Firstly, the MPC with an arbitrary energy density of 9.22 J/cm^2 was determined for both *S. aureus* and *E. coli* (Table 5). A CFU count assay was also carry out to infer if light exposure without exposure to DES-Cur had any significant effect on bacteria viability (Fig. 6A).

The lowest MPC value was obtained for *S. aureus* which is in accordance with the literature as several accounts report greater sensibility of Gram-positive bacteria to both the basal and photo-induced antibacterial effects of Cur [65, 67, 79]. Nevertheless, the value required for complete *E. coli*

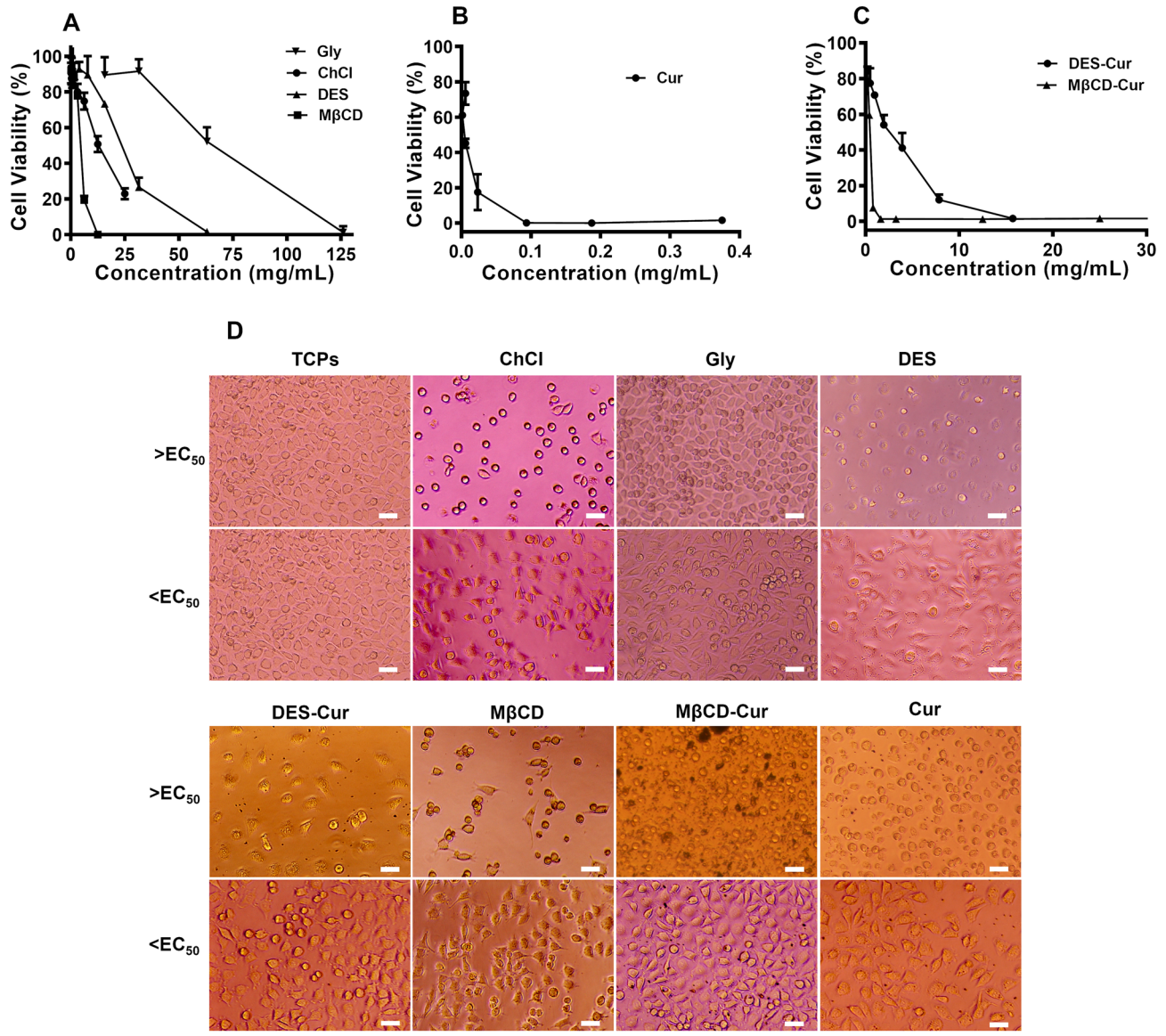

Fig. 5 A Dose–response curves of Gly, ChCl, DES and MβCD. (B) Dose–response curve of Cur. (C) Dose–response curve of DES-Cur and MβCD-Cur. (D) Morphology of L929 cells when exposed to concentrations above and below EC_{50} of the isolated compounds and Cur-based formulations tested. Scale bar is 50 µm

eradication is below the determined EC_{50} for L929 cells. Furthermore, exposure to blue light without the presence of DES-Cur showed no relevant effect on bacterial viability as no significant decrease in CFU count was observed when comparing bacteria exposed to blue light (Fig. 6A). To gain further insight into the dynamics of blue-light induced phototoxicity of DES-Cur, a bacterial viable count assay was carried out using the lowest MPC value obtained, 0.124 mg/mL, with different energy density values against both *S. aureus* and *E. coli* (Fig. 6B).

The obtained results for *E. coli* show that using DES-Cur at 0.124 mg/mL, with an energy density of 9.22 J/cm^2, a $\log_{10}$ reduction of 3.68 ± 0.26 (≈ 99.99% reduction of viable bacteria) can be achieved. This bactericidal effect is further increased at 13.82 J/cm^2, where a $\log_{10}$ reduction of 4.46 ± 0.04 (≈ 99.999% reduction of viable bacteria) was obtained. As for *S. aureus* with an energy density of 3.07 J/cm^2, a $\log_{10}$ reduction of 4.36 ± 0.14 was obtained with no colonies being observed for higher exposure (i.e., 4.61, 9.22 and 13.82 J/cm^2). These results are in accordance with the literature, emphasizing the potential of Cur as a photosensitizing agent for blue-light aPDT [60, 67, 80, 81].

Considering the results obtained in the phototoxicity assessment of DES-Cur against *E. coli* and *S. aureus,* a concentration of 0.124 mg/mL of DES-Cur was chosen to carry out phototoxicity assays against L929 Cell line. In

Table 4 EC_{50} values of isolated compounds and Cur-based formulations

	EC_{50} (mg/mL)
Isolated compounds	
Gly	65.94 ± 2.82*
ChCl	10.86 ± 0.60*
DES	22.59 ± 0.71*
MβCD	4.49 ± 0.18*
Cur	0.02 ± 0.003*
Cur-based formulations	
DES-Cur	1.83 ± 0.22$
MβCD-Cur	0.47 ± 0.05$

Statistical analysis (one-way ANOVA with tukey post-hoc) was performed, and differences considered significant for p values < 0.05

*Denotes statistically significant differences of an isolated compound when compared with all others

$Denotes statistically significant differences of Cur-based formulations when compared with each other and Cur

Table 5 MPC values with and energy density of 9.22 J/cm^2 of DES-Cur against *S. aureus* and *E. coli*

Bacteria strains	MPC (mg/mL)	[Cur]* (μg/mL)
E. coli	0.248	2.250
S. aureus	0.124	1.125

*[Cur] present in the amount of formulation employed

addition to DES-Cur, cells were also exposed to a DMEM extract with an equivalent Cur concentration. After exposure to varying energy densities, cells were observed by optic microscopy (Fig. S6). As expected, with increasing energy density cells exposed to extracts containing Cur showed a progressive loss of viability, adopting a rounder morphology with loss of adherence to the well surface. In contrast, exposure to blue light up to an energy density of 13.82 J/cm^2, in the absence of Cur, appears to have a significantly less detrimental effect on L929 cells, as they present a stretched morphology and good adherence to the well surface throughout the different energy density values. To further assess cell viability a live/dead assay was also performed (Fig. 7).

Overall, higher energy density, with exposure to a photosensitizer, leads to substantially greater photo-induced toxicity against L929 cells as can be verified by the gradual increase in compromised cells (red stained cells) and the gradual decrease of green fluorescence intensity (viable cells). This behavior was expected since several studies have reported a cytotoxic effect of Cur-based blue-light PDT on animal cells, with some approaches for cancer and hyperproliferative skin disorders being currently explored [9, 10, 82, 83]. Nevertheless, it should be noted that a few viable cells are observed even at the highest energy density value tested when exposed to the DES-Cur concentration required to achieve significant antibacterial effect. Furthermore, blue-light irradiation at an energy density of 13.82 J/cm^2, without the presence of a photosensitizer, does not significantly hamper cell viability emphasizing the low toxicity of the blue-light dosage needed for a phototherapeutic effect. Overall, the obtained results highlight the existence of a therapeutic window for the treatment of localized superficial infections, where a balance can be achieved between significant eradication of bacterial pathogens and acceptable cellular toxicity.

4 Conclusion

In this study, two vehicles were used to produce Cur formulations with enhanced solubility profile, namely MβCD and a ChCl:Gly DES and their potential as phototherapeutic agents for blue-light aPDT evaluated. The produced vehicles were able to successfully solubilize Cur and significantly enhance its solubility in aqueous media. Overall, it was possible to verify that complexation with MβCD appears to hinder some of Cur's basal biological properties (i.e., antibacterial and

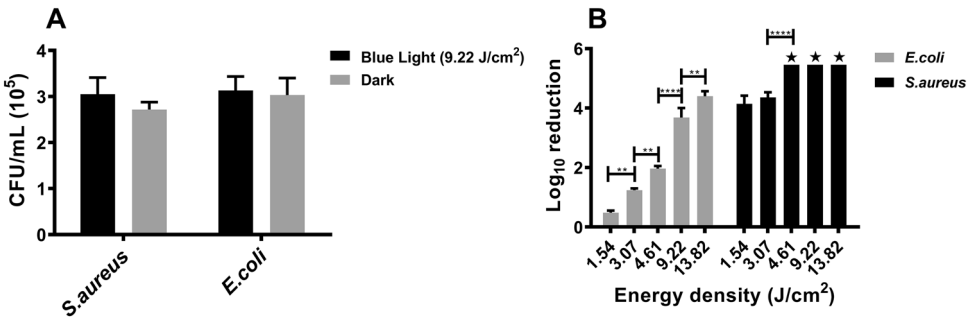

Fig. 6 **A** CFU/mL values of *S. aureus* and *E. coli* bacterial suspension after blue-light irradiation or when kept in the dark for 30 min. **B** Log_{10} reduction values of bacteria exposed to 0.124 mg/mL of DES-Cur at varying energy densities. Statistical analysis (one-way ANOVA with tukey post-hoc) was performed: $p < 0.0$ 1(**), $p < 0.0001$ (****). ★No colonies were observed so a log_{10} reduction ≥ 5.485 was considered

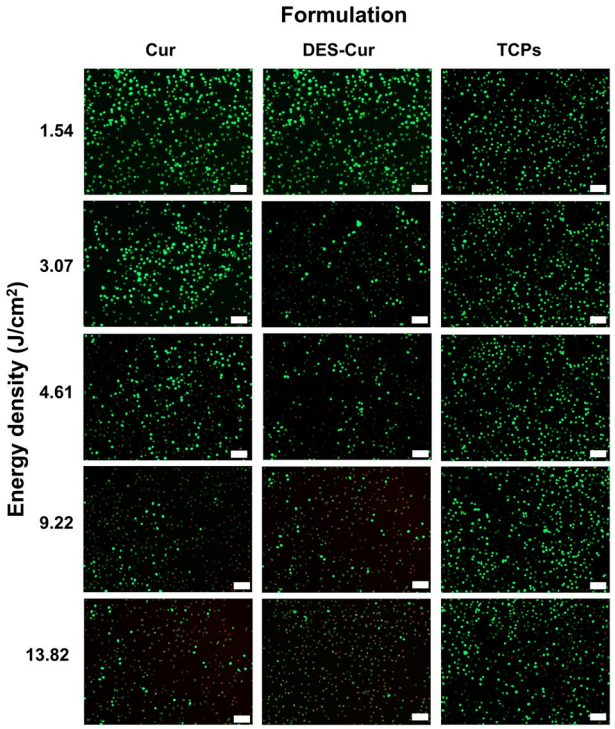

Fig. 7 Live/dead assay of L929 cells when exposed to 0.124 mg/mL of DES-Cur and 1.125 µg/mL of Cur (concentration equivalent to DES-Cur) at different energy densities. Cells irradiated in the absence of these compounds (TCPs) were also included. TCPs – Tissue culture polystyrene. Scale bar is 100 µm

antioxidant) when compared with the dissolution in DES or organic solvents. Furthermore, MβCD-Cur was shown to be less photo-responsive than DES-Cur, which may hamper its application in PDT approaches. Ultimately, DES-Cur proved superior for phototherapeutic applications due to displaying greater biological and photo-responsive properties (i.e., antioxidant, antibacterial and phototoxicity) than MβCD-Cur. Overall, this study found DES to be the more effective vehicle for Cur in terms of phototherapeutic potential which will serve as basis to develop novel platforms and approaches for blue-light PDT targeting localized superficial infections.

Supplementary Information The online version contains supplementary material available at https://doi.org/10.1007/s43630-022-00197-0.

Author contributions Conceptualization: JMS and ES; data curation: ES, JMS and IMA; investigation, ES JMS and RLR; methodology: ES and JMS; supervision: JMS and RLR; writing—original draft: ES, JMS and RLR; writing—review and editing: JMS and RLR; All authors have read and agreed to the published version of the manuscript

Funding This work received funding from Foundation for Science and Technology (FCT), through the doctoral grant with reference number SFRH/BD/143902/2019. J.M.S. would also like to acknowledge the financial support by the FCT through the post-doctoral contract with reference number CCEEIND/01026/2018.

Declarations

Conflict of interest The authors have no relevant financial or non-financial interests to disclose.

Consent of publication All authors agree with the publication of this manuscript.

References

1. Dias, D. A., Urban, S., & Roessner, U. (2012). A historical overview of natural products in drug discovery. *Metabolites, 2*(2), 303–336. https://doi.org/10.3390/metabo2020303
2. Ji, H. F., Li, X. J., & Zhang, H. Y. (2009). Natural products and drug discovery: Can thousands of years of ancient medical knowledge lead us to new and powerful drug combinations in the fight against cancer and dementia? *EMBO Reports, 10*(3), 194–200. https://doi.org/10.1038/embor.2009.12
3. González-Albadalejo, J., Sanz, D., Claramunt, R. M., Lavandera, J. L., Alkorta, I., & Elguero, J. (2015). Curcumin and curcuminoids: Chemistry, structural studies and biological properties. *An Real Acad Nac Farm., 81*, 278–310.
4. Joe, B., Vijaykumar, M., & Lokesh, B. (2004). Biological properties of curcumin-cellular and molecular mechanisms of action. *Critical Reviews in Food Science and Nutrition, 44*(2), 97–111. https://doi.org/10.1080/10408690490424702
5. Kharat, M., Du, Z., Zhang, G., & McClements, D. J. (2017). Physical and chemical stability of curcumin in aqueous solutions and emulsions: Impact of pH, temperature, and molecular environment. *Journal of Agriculture and Food Chemistry, 65*(8), 1525–1532. https://doi.org/10.1021/acs.jafc.6b04815
6. Peng, S., Li, Z., Zou, L., Liu, W., Liu, C., & McClements, D. J. (2018). Improving curcumin solubility and bioavailability by encapsulation in saponin-coated curcumin nanoparticles prepared using a simple pH-driven loading method. *Food & Function, 9*(3), 1829–1839. https://doi.org/10.1039/c7fo01814b
7. Dias, L. D., Blanco, K. C., Mfouo-Tynga, I. S., Inada, N. M., & Bagnato, V. S. (2020). Curcumin as a photosensitizer: From molecular structure to recent advances in antimicrobial photodynamic therapy. *Journal of Photochemistry and Photobiology C: Photochemistry Reviews*. https://doi.org/10.1016/j.jphotochemrev.2020.100384
8. Hegge, A. B., Bruzell, E., Kristensen, S., & Tønnesen, H. (2012). Photoinactivation of Staphylococcus epidermidis biofilms and suspensions by the hydrophobic photosensitizer curcumin–effect of selected nanocarrier: Studies on curcumin and curcuminoides XLVII. *European Journal of Pharmaceutical Sciences, 47*(1), 65–74. https://doi.org/10.1016/j.ejps.2012.05.002
9. Ellerkamp, V., Bortel, N., Schmid, E., Kirchner, B., Armeanu-Ebinger, S., & Fuchs, J. (2016). Photodynamic therapy potentiates the effects of curcumin on pediatric epithelial liver tumor cells. *Anticancer Research, 36*(7), 3363–3372.
10. Hak, A., Shinde, V. R., & Rengan, A. K. (2021). A review of advanced nanoformulations in phototherapy for cancer therapeutics. *Photodiagnosis and Photodynamic Therapy*. https://doi.org/10.1016/j.pdpdt.2021.102205
11. Cieplik, F., Deng, D., Crielaard, W., Buchalla, W., Hellwig, E., Al-Ahmad, A., et al. (2018). Antimicrobial photodynamic therapy–What we know and what we don't. *Critical Reviews in Microbiology, 44*(5), 571–589. https://doi.org/10.1080/1040841X.2018.1467876
12. Ribeiro, M. S., Sabino, C. P., & Núñez, S. C. (2019). Antimicrobial photodynamic therapy: from basis to clinical applications. In:

17th International Photodynamic Association World Congress: International Society for Optics and Photonics (vol. 11070, p. 1107048)
13. Carrera, E., Dias, H., Corbi, S., Marcantonio, R., Bernardi, A., Bagnato, V., et al. (2016). The application of antimicrobial photodynamic therapy (aPDT) in dentistry: A critical review. *Laser Physics, 26*(12), 123001. https://doi.org/10.1088/1054-660X/26/12/123001
14. Sun, Y., Geng, X., Wang, Y., Su, X., Han, R., Wang, J., et al. (2021). Highly efficient water-soluble photosensitizer based on chlorin: Synthesis, characterization, and evaluation for photodynamic therapy. *ACS Pharmacology & Translational Science, 4*(2), 802–812. https://doi.org/10.1021/acsptsci.1c00004
15. Altunbas, A., Lee, S. J., Rajasekaran, S. A., Schneider, J. P., & Pochan, D. J. (2011). Encapsulation of curcumin in self-assembling peptide hydrogels as injectable drug delivery vehicles. *Biomaterials, 32*(25), 5906–5914. https://doi.org/10.1016/j.biomaterials.2011.04.069
16. Mangolim, C. S., Moriwaki, C., Nogueira, A. C., Sato, F., Baesso, M. L., Neto, A. M., et al. (2014). Curcumin–β-cyclodextrin inclusion complex: Stability, solubility, characterisation by FT-IR, FT-Raman, X-ray diffraction and photoacoustic spectroscopy, and food application. *Food Chemistry, 153*, 361–370. https://doi.org/10.1016/j.foodchem.2013.12.067
17. Yadav, S., Singh, A. K., Agrahari, A. K., Sharma, K., Singh, A. S., Gupta, M. K., et al. (2020). Making of water soluble curcumin to potentiate conventional antimicrobials by inducing apoptosis-like phenomena among drug-resistant bacteria. *Science and Reports, 10*(1), 1–22. https://doi.org/10.1038/s41598-020-70921-2
18. Yallapu, M. M., Jaggi, M., & Chauhan, S. C. (2010). β-Cyclodextrin-curcumin self-assembly enhances curcumin delivery in prostate cancer cells. *Colloids and Surfaces B, 79*(1), 113–125. https://doi.org/10.1016/j.colsurfb.2010.03.039
19. Kurkov, S. V., & Loftsson, T. (2013). Cyclodextrins. *International Journal of Pharmaceutics, 453*(1), 167–180. https://doi.org/10.1016/j.ijpharm.2012.06.055
20. Karpkird, T., Khunsakorn, R., Noptheeranuphap, C., & Midpanon, S. (2018). Inclusion complexes and photostability of UV filters and curcumin with beta-cyclodextrin polymers: Effect on cross-linkers. *Journal of Inclusion Phenomena and Macrocyclic Chemistry, 91*(1), 37–45. https://doi.org/10.1007/s10847-018-0796-y
21. Jeliński, T., Przybyłek, M., & Cysewski, P. (2019). Natural deep eutectic solvents as agents for improving solubility, stability and delivery of curcumin. *Pharmaceutical Research, 36*(8), 1–10. https://doi.org/10.1007/s11095-019-2643-2
22. Shekaari, H., Mokhtarpour, M., Faraji, S., & Zafarani-Moattar, M. T. (2021). Enhancement of curcumin solubility by some choline chloride-based deep eutectic solvents at different temperatures. *Fluid Phase Equilibria, 532*, 112917. https://doi.org/10.1016/j.fluid.2020.112917
23. Abbott, A. P., Boothby, D., Capper, G., Davies, D. L., & Rasheed, R. K. (2004). Deep eutectic solvents formed between choline chloride and carboxylic acids: Versatile alternatives to ionic liquids. *Journal of the American Chemical Society, 126*(29), 9142–9147. https://doi.org/10.1021/ja048266j
24. Paiva, A., Craveiro, R., Aroso, I., Martins, M., Reis, R. L., & Duarte, A. R. C. (2014). Natural deep eutectic solvents–solvents for the 21st century. *ACS Sustainable Chemistry & Engineering, 2*(5), 1063–1071. https://doi.org/10.1021/sc500096j
25. Aroso, I. M., Craveiro, R., Rocha, Â., Dionísio, M., Barreiros, S., Reis, R. L., et al. (2015). Design of controlled release systems for THEDES—Therapeutic deep eutectic solvents, using supercritical fluid technology. *International Journal of Pharmaceutics, 492*(1–2), 73–79. https://doi.org/10.1016/j.ijpharm.2015.06.038
26. Roda, A., Santos, F., Matias, A. A., Paiva, A., & Duarte, A. R. C. (2020). Design and processing of drug delivery formulations of therapeutic deep eutectic systems for tuberculosis. *Journal of Supercritical Fluids, 161*, 104826. https://doi.org/10.1016/j.supflu.2020.104826
27. Silva, J. M., Pereira, C. V., Mano, F., Silva, E., Castro, V. N. I., Sá-Nogueira, I., et al. (2019). Therapeutic role of deep eutectic solvents based on menthol and saturated fatty acids on wound healing. *ACS Applied Bio Materials., 2*(10), 4346–4355. https://doi.org/10.1021/acsabm.9b00598
28. Marcus, Y. (2019). *Applications of deep eutectic solvents. Deep eutectic solvents* (pp. 111–151). Springer International Publishing.
29. Shishov, A., Bulatov, A., Locatelli, M., Carradori, S., & Andruch, V. (2017). Application of deep eutectic solvents in analytical chemistry A review. *Microchemical Journal, 135*, 33–38. https://doi.org/10.1016/j.microc.2017.07.015
30. Anastas, P. T., & Warner, J. C. (1998). Green chemistry. *Frontiers, 640*, 1998.
31. Yadav, V. R., Suresh, S., Devi, K., & Yadav, S. (2009). Effect of cyclodextrin complexation of curcumin on its solubility and antiangiogenic and anti-inflammatory activity in rat colitis model. *An Official Journal of the American Association of Pharmaceutical Scientists, 10*(3), 752–762. https://doi.org/10.1208/s12249-009-9264-8
32. Fonseca-Santos, B., Gremião, M. P. D., & Chorilli, M. (2017). A simple reversed phase high-performance liquid chromatography (HPLC) method for determination of in situ gelling curcumin-loaded liquid crystals in in vitro performance tests. *Arabian Journal of Chemistry, 10*(7), 1029–1037. https://doi.org/10.1016/j.arabjc.2016.01.014
33. Molyneux, P. (2004). The use of the stable free radical diphenylpicrylhydrazyl (DPPH) for estimating antioxidant activity. *Songklanakarin Journal of Science and Technology, 26*(2), 211–219.
34. Aroso, I. M., Paiva, A., Reis, R. L., & Duarte, A. R. C. (2017). Natural deep eutectic solvents from choline chloride and betaine–Physicochemical properties. *Journal of Molecular Liquids, 241*, 654–661. https://doi.org/10.1016/j.molliq.2017.06.051
35. Morrison, H. G., Sun, C. C., & Neervannan, S. (2009). Characterization of thermal behavior of deep eutectic solvents and their potential as drug solubilization vehicles. *International Journal of Pharmaceutics, 378*(1–2), 136–139. https://doi.org/10.1016/j.ijpharm.2009.05.039
36. Pereira, C. V., Silva, J. M., Rodrigues, L., Reis, R. L., Paiva, A., Duarte, A. R. C., et al. (2019). Unveil the anticancer potential of limomene based therapeutic deep eutectic solvents. *Science and Reports, 9*(1), 1–11. https://doi.org/10.1038/s41598-019-51472-7
37. Pedro, S. N., Freire, M. G., Freire, C. S., & Silvestre, A. J. (2019). Deep eutectic solvents comprising active pharmaceutical ingredients in the development of drug delivery systems. *Expert Opinion on Drug Delivery, 16*(5), 497–506. https://doi.org/10.1080/17425247.2019.1604680
38. Elderderi, S., Leman-Loubiere, C., Wils, L., Henry, S., Bertrand, D., Byrne, H. J., et al. (2020). ATR-IR spectroscopy for rapid quantification of water content in deep eutectic solvents. *Journal of Molecular Liquids, 311*, 113361. https://doi.org/10.1016/j.molliq.2020.113361
39. Banjare, M. K., Behera, K., Satnami, M. L., Pandey, S., & Ghosh, K. K. (2018). Self-assembly of a short-chain ionic liquid within deep eutectic solvents. *RSC Advances, 8*(15), 7969–7979. https://doi.org/10.1039/C7RA13557B
40. Gautam, R., Kumar, N., & Lynam, J. G. (2020). Theoretical and experimental study of choline chloride-carboxylic acid deep eutectic solvents and their hydrogen bonds. *Journal of Molecular Structure, 1222*, 128849. https://doi.org/10.1016/j.molstruc.2020.128849
41. Zhu, S., Li, H., Zhu, W., Jiang, W., Wang, C., Wu, P., et al. (2016). Vibrational analysis and formation mechanism of typical deep

eutectic solvents: An experimental and theoretical study. *Journal of Molecular Graphics and Modelling, 68*, 158–175. https://doi.org/10.1016/j.jmgm.2016.05.003
42. Lim, C. Y., Majid, M. F., Rajasuriyan, S., Mohd Zaid, H. F., Jumbri, K., & Chong, F. K. (2020). Desulfurization performance of choline chloride-based deep eutectic solvents in the presence of graphene oxide. *Environments, 7*(11), 97. https://doi.org/10.3390/environments7110097
43. Basar, A. O., Prieto, C., Durand, E., Villeneuve, P., Sasmazel, H. T., & Lagaron, J. (2020). Encapsulation of β-carotene by emulsion electrospraying using deep eutectic solvents. *Molecules, 25*(4), 981. https://doi.org/10.3390/molecules25040981
44. Ahmadi, R., Hemmateenejad, B., Safavi, A., Shojaeifard, Z., Shahsavar, A., Mohajeri, A., et al. (2018). Deep eutectic–water binary solvent associations investigated by vibrational spectroscopy and chemometrics. *Physical Chemistry Chemical Physics: PCCP, 20*(27), 18463–18473. https://doi.org/10.1039/c8cp00409a
45. Ribeiro, A., Figueiras, A., Santos, D., & Veiga, F. (2008). Preparation and solid-state characterization of inclusion complexes formed between miconazole and methyl-β-cyclodextrin. *An Official Journal of the American Association of Pharmaceutical Scientists, 9*(4), 1102–1109. https://doi.org/10.1208/s12249-008-9143-8
46. Abdullah, G. H., & Kadhom, M. A. (2016). Studying of two choline chloride's deep eutectic solvents in their aqueous mixtures. *International Journal of Engineering Research and Development, 12*(9), 73–80. https://doi.org/10.1007/s13369-017-2431-4
47. Janicka, P., Przyjazny, A., & Boczkaj, G. (2021). Novel, "acid tuned" deep eutectic solvents based on protonated L-proline. *Journal of Molecular Liquids, 333*, 115965. https://doi.org/10.1016/j.molliq.2021.115965
48. Gygli, G., Xu, X., & Pleiss, J. (2020). Meta-analysis of viscosity of aqueous deep eutectic solvents and their components. *Science and Reports, 10*(1), 1–11. https://doi.org/10.15490/FAIRDOMHUB.1.STUDY.767.1
49. Schneider, C., Gordon, O. N., Edwards, R. L., & Luis, P. B. (2015). Degradation of curcumin: From mechanism to biological implications. *Journal of Agriculture and Food Chemistry, 63*(35), 7606–7614. https://doi.org/10.1021/acs.jafc.5b00244
50. Sharma, V., & Pathak, K. (2016). Effect of hydrogen bond formation/replacement on solubility characteristics, gastric permeation and pharmacokinetics of curcumin by application of powder solution technology. *Acta Pharmaceutica Sinica B, 6*(6), 600–613. https://doi.org/10.1016/j.apsb.2016.05.015
51. Neuberg, C. (1916). Hydrotropic phenomena. *Biochemische Zeitschrift, 76*(1), 107–108.
52. Cláudio, A. F. M., Neves, M. C., Shimizu, K., Lopes, J. N. C., Freire, M. G., & Coutinho, J. A. (2015). The magic of aqueous solutions of ionic liquids: Ionic liquids as a powerful class of catanionic hydrotropes. *Green Chemistry, 17*(7), 3948–3963. https://doi.org/10.1039/C5GC00712G
53. Soares, B., da Costa Lopes, A. M., Silvestre, A. J., Pinto, P. C. R., Freire, C. S., & Coutinho, J. A. (2021). Wood delignification with aqueous solutions of deep eutectic solvents. *Industrial Crops and Products, 160*, 113128. https://doi.org/10.1016/j.indcrop.2020.113128
54. Soares, B., Tavares, D. J., Amaral, J. L., Silvestre, A. J., Freire, C. S., & Coutinho, J. O. A. (2017). Enhanced solubility of lignin monomeric model compounds and technical lignins in aqueous solutions of deep eutectic solvents. *ACS Sustainable Chemistry & Engineering., 5*(5), 4056–4065. https://doi.org/10.1021/acssuschemeng.7b00053
55. Mondal, S., Ghosh, S., & Moulik, S. P. (2016). Stability of curcumin in different solvent and solution media: UV–visible and steady-state fluorescence spectral study. *Journal of Photochemistry and Photobiology B: Biology, 158*, 212–218. https://doi.org/10.1016/j.jphotobiol.2016.03.004
56. Priyadarsini, K. I. (2014). The chemistry of curcumin: From extraction to therapeutic agent. *Molecules, 19*(12), 20091–20112. https://doi.org/10.3390/molecules191220091
57. Kim, H.-J., Kim, D.-J., Karthick, S., Hemalatha, K., Raj, C. J., Ok, S., et al. (2013). Curcumin dye extracted from *Curcuma longa* L. used as sensitizers for efficient dye-sensitized solar cells. *International Journal of Electrochemical Science, 8*(6), 8320–8328.
58. Van Nong, H., Hung, L. X., Thang, P. N., Chinh, V. D., Dung, P. T., Van Trung, T., et al. (2016). Fabrication and vibration characterization of curcumin extracted from turmeric (*Curcuma longa*) rhizomes of the northern Vietnam. *Springerplus, 5*(1), 1–9. https://doi.org/10.1186/s40064-016-2812-2
59. Ben Mihoub, A., Acherar, S., Frochot, C., Malaplate, C., Yen, F. T., & Arab-Tehrany, E. (2021). Synthesis of new water soluble β-Cyclodextrin@ curcumin conjugates and in vitro safety evaluation in primary cultures of rat cortical neurons. *International Journal of Molecular Sciences, 22*(6), 3255. https://doi.org/10.3390/ijms22063255
60. Wikene, K. O., Bruzell, E., & Tønnesen, H. H. (2015). Characterization and antimicrobial phototoxicity of curcumin dissolved in natural deep eutectic solvents. *European Journal of Pharmaceutical Sciences, 80*, 26–32. https://doi.org/10.1016/j.ejps.2015.09.013
61. d'Agostino, S., Azzali, A., Casali, L., Taddei, P., & Grepioni, F. (2020). Environmentally friendly sunscreens: Mechanochemical synthesis and characterization of β-CD inclusion complexes of avobenzone and octinoxate with improved photostability. *ACS Sustainable Chemistry & Engineering, 8*(35), 13215–13225. https://doi.org/10.1021/acssuschemeng.0c02735
62. Karpkird, T., Khunsakorn, R., Noptheeranuphap, C., & Jettanasen, J. (2016). Photostability of water-soluble inclusion complexes of UV-filters and curcumin with gamma-cyclodextrin polymer. *Journal of Inclusion Phenomena and Macrocyclic Chemistry, 84*(1–2), 121–128. https://doi.org/10.1007/s10847-015-0589-5
63. Teow, S. Y., Liew, K., Ali, S. A., Khoo, A.S.-B., & Peh, S.-C. (2016). Antibacterial action of curcumin against *Staphylococcus aureus*: a brief review. *Journal of Tropical Medicine*. https://doi.org/10.1155/2016/2853045
64. Zheng, D., Huang, C., Huang, H., Zhao, Y., Khan, M. R. U., Zhao, H., et al. (2020). Antibacterial mechanism of curcumin: A review. *Chemistry & Biodiversity, 17*(8), e2000171. https://doi.org/10.1002/cbdv.202000171
65. Gunes, H., Gulen, D., Mutlu, R., Gumus, A., Tas, T., & Topkaya, A. E. (2016). Antibacterial effects of curcumin: An in vitro minimum inhibitory concentration study. *Toxicology and Industrial Health, 32*(2), 246–250. https://doi.org/10.1177/0748233713498458
66. Silhavy, T. J., Kahne, D., & Walker, S. (2010). The bacterial cell envelope. *Cold Spring Harbor Perspectives in Biology, 2*(5), a000414. https://doi.org/10.1101/cshperspect.a000414
67. Hegge, A. B., Andersen, T., Melvik, J. E., Bruzell, E., Kristensen, S., & Tønnesen, H. H. (2011). Formulation and bacterial phototoxicity of curcumin loaded alginate foams for wound treatment applications: Studies on curcumin and curcuminoides XLII. *Journal of Pharmaceutical Sciences, 100*(1), 174–185. https://doi.org/10.1002/jps.22263
68. Santos, R. S., Figueiredo, C., Azevedo, N. F., Braeckmans, K., & De Smedt, S. C. (2018). Nanomaterials and molecular transporters to overcome the bacterial envelope barrier: Towards advanced delivery of antibiotics. *Advanced Drug Delivery Reviews, 136*, 28–48. https://doi.org/10.1016/j.addr.2017.12.010
69. Sakuragi, M., Maeda, E., & Kusakabe, K. (2020). Penetration process of a hydrated deep eutectic solvent through the *Stratum*

corneum and its application as a protein penetration enhancer. *ChemistryOpen., 9*(9), 953.
70. Xu, P., Du, P.-X., Zong, M.-H., Li, N., & Lou, W.-Y. (2016). Combination of deep eutectic solvent and ionic liquid to improve biocatalytic reduction of 2-octanone with *Acetobacter pasteurianus* GIM1. 158 cell. *Scientific Reports, 6*(1), 1–10.
71. Li, Z., & Lee, P. I. (2016). Investigation on drug solubility enhancement using deep eutectic solvents and their derivatives. *International Journal of Pharmaceutics, 505*(1–2), 283–288. https://doi.org/10.1016/j.ijpharm.2016.04.018
72. Matilainen, L., Toropainen, T., Vihola, H., Hirvonen, J., Järvinen, T., Jarho, P., et al. (2008). In vitro toxicity and permeation of cyclodextrins in Calu-3 cells. *Journal of Controlled Release, 126*(1), 10–16. https://doi.org/10.1016/j.jconrel.2007.11.003
73. Mundhara, N., Majumder, A., & Panda, D. (2019). Methyl-β-cyclodextrin, an actin depolymerizer augments the antiproliferative potential of microtubule-targeting agents. *Science and Reports, 9*(1), 1–12. https://doi.org/10.1038/s41598-019-43947-4
74. Radošević, K., Bubalo, M. C., Srček, V. G., Grgas, D., Dragičević, T. L., & Redovniković, I. R. (2015). Evaluation of toxicity and biodegradability of choline chloride based deep eutectic solvents. *Ecotoxicology and Environmental Safety, 112*, 46–53. https://doi.org/10.1016/j.ecoenv.2014.09.034
75. Macário, I., Oliveira, H., Menezes, A., Ventura, S., Pereira, J., Gonçalves, A., et al. (2019). Cytotoxicity profiling of deep eutectic solvents to human skin cells. *Science and Reports, 9*(1), 1–9. https://doi.org/10.1038/s41598-019-39910-y
76. Hayyan, M., Hashim, M. A., Hayyan, A., Al-Saadi, M. A., AlNashef, I. M., Mirghani, M. E. S., et al. (2013). Are deep eutectic solvents benign or toxic? *Chemosphere, 90*(7), 2193–2195. https://doi.org/10.1016/j.chemosphere.2012.11.004
77. Cooper, G. M., Hausman, R. E., & Hausman, R. E. (2007). *The cell: A molecular approach*. ASM Press.
78. Hammoud, Z., Khreich, N., Auezova, L., Fourmentin, S., Elaissari, A., & Greige-Gerges, H. (2019). Cyclodextrin-membrane interaction in drug delivery and membrane structure maintenance. *International Journal of Pharmaceutics, 564*, 59–76. https://doi.org/10.1016/j.ijpharm.2019.03.063
79. Tyagi, P., Singh, M., Kumari, H., Kumari, A., & Mukhopadhyay, K. (2015). Bactericidal activity of curcumin I is associated with damaging of bacterial membrane. *PLoS ONE, 10*(3), e0121313. https://doi.org/10.1371/journal.pone.0121313
80. Freitas, M. A., Pereira, A. H., Pinto, J. G., Casas, A., & Ferreira-Strixino, J. (2019). Bacterial viability after antimicrobial photodynamic therapy with curcumin on multiresistant Staphylococcus aureus. *Future Microbiology, 14*(9), 739–748. https://doi.org/10.2217/fmb-2019-0042
81. Haukvik, T., Bruzell, E., Kristensen, S., & Tønnesen, H. (2009). Photokilling of bacteria by curcumin in different aqueous preparations. Studies on curcumin and curcuminoids XXXVII. *Die Pharmazie, 64*(10), 666–673. https://doi.org/10.1691/ph.2009.0000
82. Carrion-Gutierrez, M., Ramirez-Bosca, A., Navarro-Lopez, V., Martinez-Andres, A., Asín-Llorca, M., Bernd, A., et al. (2015). Effects of Curcuma extract and visible light on adults with plaque psoriasis. *European Journal of Dermatology, 25*(3), 240–246. https://doi.org/10.1684/ejd.2015.2584
83. Liebmann, J., Born, M., & Kolb-Bachofen, V. (2010). Blue-light irradiation regulates proliferation and differentiation in human skin cells. *Journal of Investigative Dermatology, 130*(1), 259–269. https://doi.org/10.1038/jid.2009.194

Authors and Affiliations

Eduardo Silva[1,2] · Ivo M. Aroso[1,2] · Joana M. Silva[1,2] · Rui L. Reis[1,2]

[1] 3B's Research Group, I3Bs-Research Institute on Biomaterials, Biodegradables and Biomimetics, Headquarters of the European Institute of Excellence on Tissue Engineering and Regenerative Medicine, University of Minho, Avepark, Zona Industrial da Gandra, 4805-017 Barco GMR, Portugal

[2] ICVS/3B's PT Government Associated Laboratory, Braga, Guimarães, Portugal